

Journal of Biomedical Optics

SPIEDigitalLibrary.org/jbo

Effects of hypoxia on cochlear blood flow in mice evaluated using Doppler optical microangiography

Suzan Dziennis
Roberto Reif
Zhongwei Zhi
Alfred L. Nuttall
Ruikang K. Wang

Effects of hypoxia on cochlear blood flow in mice evaluated using Doppler optical microangiography

Suzan Dziennis,^{a*} Roberto Reif,^{a*} Zhongwei Zhi,^a Alfred L. Nuttall,^b and Ruikang K. Wang^{a*}

^aUniversity of Washington, Department of Bioengineering, 3720 15th Avenue N.E., Seattle, Washington 98195

^bOregon Health and Science University, Oregon Hearing Research Center, School of Medicine, Portland, Oregon 97239

Abstract. Reduced cochlear blood flow (CoBF) is a main contributor to hearing loss. Studying CoBF has remained a challenge due to the lack of available tools. Doppler optical microangiography (DOMAG), a method to quantify single-vessel absolute blood flow, and laser Doppler flowmetry (LDF), a method for measuring the relative blood flow within a large volume of tissue, were used for determining the changes in CoBF due to systemic hypoxia in mice. DOMAG determined the change in blood flow in the apical turn (AT) with single-vessel resolution, while LDF averaged the change in the blood flow within a large volume of the cochlea (hemisphere with ~1 to 1.5 mm radius). Hypoxia was induced by decreasing the concentration of oxygen-inspired gas, so that the oxygen saturation was reduced from >95% to ~80%. DOMAG determined that during hypoxia the blood flow in two areas of the AT near and far from the helicotrema were increased and decreased, respectively. The LDF detected a decrease in blood flow within a larger volume of the cochlea (several turns averaged together). Therefore, the use of DOMAG as a tool for studying cochlear blood flow due to its ability to determine absolute flow values with single-vessel resolution was proposed. © 2012 Society of Photo-Optical Instrumentation Engineers (SPIE). [DOI: 10.1117/1.JBO.17.10.106003]

Keywords: cochlear blood flow; hypoxia; Doppler optical microangiography.

Paper 12366 received Jun. 11, 2012; revised manuscript received Aug. 28, 2012; accepted for publication Aug. 30, 2012; published online Oct. 1, 2012.

1 Introduction

In 2006 it was estimated that more than 642 million people worldwide had some form of hearing deficit.¹ Inadequate blood supply, or ischemia, in the cochlea is a contributor to hearing loss,² and abnormal regulation of cochlear blood flow (CoBF) is involved in noise-induced hearing loss, endolymphatic hydrops and presbycusis.³ Moreover, diseases that cause hypoperfusion or ischemia, such as embolism and vascular disease, could also induce hearing loss.^{4,5} Therefore, studying the cochlear microvasculature is important in developing clinical therapeutics to improve or prevent hearing loss due to ischemia.

The cochlea contains the organ of Corti, which translates sound into nerve impulses that travel to the brain. With its high metabolic demand, maintaining normal blood flow to the cochlea is necessary for generating the ionic concentrations required for auditory transduction. Normal CoBF is important for maintaining ion and fluid balance in the inner ear and the endocochlear potential. Also, the cochlea is vulnerable to ischemia.³ Providing the main blood supply to the cochlea is the spiral modiolar artery, a terminal branch of the anterior inferior cerebellar artery; this artery has radial branches to the cochlear lateral wall that form two major capillary systems, one in the spiral ligament and the other in the stria vascularis. The microcirculatory (capillary) blood flow in the stria vascularis is responsible for ion pumping and the endocochlear potential. Previous reports using laser Doppler flowmetry (LDF) and oxygen-sensitive microelectrodes show different effects of CoBF in response to hypoxia,⁶⁻⁹ with the mean velocity of blood flow in

spiral ligament vessels measured at 0.12 mm/s, while stria vascularis velocity was measured at 0.08 mm/s.¹⁰ It has been demonstrated that high intensity sound exposure produces a decline in cochlear blood flow.⁹

Unfortunately, the ability to investigate the CoBF, both clinically and experimentally, is challenging due to the difficulties in accessing the inner ear and the cochlea. Currently, there are a number of methods used for studying blood flow in biological tissues. Commonly used techniques, such as LDF, measure only relative rather than absolute changes in blood flow and the measurement volume cannot be determined.^{11,12} LDF is a commonly used technique for flow measurements (number of red blood cells in a given volume multiplied by their mean velocity); however, it does not provide sufficient spatial resolution, and is not capable of providing a three-dimensional (3-D) map of the vasculature. LDF has previously been used to measure the changes in CoBF during occlusion of the stapedial artery (SA) and anterior inferior cerebellar artery,¹³ topical application of a vasodilators,¹⁴ and loud sound exposure.^{9,15} Also, dye dilution¹⁶ is a technique based on monitoring the flow of exogenous fluorescent dyes, however, the injection is invasive and may provoke side effects.

Optical microangiography (OMAG) is a new imaging modality based on optical coherence tomography (OCT),¹⁷⁻²² which allows non-invasive measurement of the 3-D microstructural and microvascular composition of biological tissues, such as the brain²³ and eyes.²⁴ OCT and OMAG have previously been used to image the cochlea *in vivo*.²⁵⁻²⁷ When combined with the Doppler effect of flowing particles on the frequency of the light, OCT has been extended to include imaging of blood flow in tissue. The most commonly used OCT method

*These authors have contributed equally to this work.

Address all correspondence to: Ruikang K. Wang, University of Washington, Department of Bioengineering, 3720 15th Avenue N.E., Seattle, Washington 98195. Tel: 206 616 5025; Fax: 206 685 3300; E-mail: wangrk@uw.edu

for measuring blood flow is the phase-resolved Doppler OCT.^{28,29} Subsequently, OMAG was combined with phase-resolved Doppler OCT to produce a method called Doppler OMAG (DOMAG), which has extended OMAG's capabilities to quantitatively measure blood flow velocity in the axial direction.³⁰ DOMAG has a higher signal-to-noise ratio and a higher performance for velocity estimation compared to phase-resolved Doppler OCT.³⁰

In the current study we used DOMAG to examine changes in CoBF in mice anesthetized with isoflurane and subjected to decreased oxygen concentration to cause severe systemic hypoxia ($SpO_2 \sim 80\%$). Using DOMAG we demonstrate that the vasculature within the cochlea is sensitive to the changes in oxygen concentration and highly regulated in order to maintain metabolic homeostasis. We compared the results with LDF that averaged the changes in total blood flow within a large volume of tissue.

2 Materials and Methods

All experiments were carried out in accordance with National Institutes of Health guidelines for research animal care and the protocols were approved by the Institutional Animal Care and Use Committee at the University of Washington. Male mice C57BL/6J (Charles River Laboratories, Hollister, CA) approximately six to seven weeks of age with body weights from 19 to 24 g were used in all experiments.

2.1 Surgical Exposure of the Cochlea in Mice

Mice were anesthetized with 1.5% isoflurane in oxygen-enriched air (20% oxygen/80% medical air) by face mask. The body temperature was maintained at $37 \pm 0.1^\circ\text{C}$ with a feedback rectal probe and heating pad (Harvard Apparatus). The head of the mouse was immobilized onto an imaging platform to minimize movement so that the left cochlea was exposed ventrally through the neck, as previously described.^{27,31} An incision was made down the midline of the neck and the left submandibular gland and posterior belly of the digastric muscle were removed by cauterization. The external carotid artery was

ligated inferior to the bifurcation. The positions of hypoglossal and facial nerves and the sternocleidomastoid muscles were used to identify the location of the bony bulla that covers the cochlea. The bulla was exposed and a 30-g needle was used to make a hole in the bulla removing the tympanic membrane to expose the cochlea, including the SA, which lies over the edge of the round window niche [Fig. 1(b)].

2.2 Flow Measurements with Doppler Optical Microangiography

A spectral domain OCT system has previously been developed³² and is presented in Fig. 1(a). The system contained a superluminescent diode light source, with a central wavelength of 1310 nm and a bandwidth of 56 nm with the theoretical axial resolution (in the Z-direction) placed at $\sim 13 \mu\text{m}$ in air. The light was divided into two arms using a 2×2 optical coupler. The light in one arm was back-reflected by the mirror (this is called the reference arm), and the light in the other arm was back-reflected by the sample (cochlea)—this is called the sample arm. In the sample arm, the light was coupled into a custom-designed optical system, which contained a collimator, a pair of galvo mirrors, and an objective lens with a 30-mm focal length. The lateral resolution (in the X and Y-direction) was $\sim 12 \mu\text{m}$. The light reflected from the sample and reference arm were recombined, and then transmitted to a home-built spectrometer that had a spectral resolution of 0.141 nm, which provided an imaging depth of 2.2 mm into the sample. A high speed InGaAs line scan camera (SUI, Goodrich Corp) was used to capture the data. The system sensitivity, defined as $S = 20 \log(M/N)$, where M is the signal obtained from a perfectly reflecting mirror and N is the noise of the system,³³ was determined to be 105 dB at a depth of 0.5 mm from the position where the distance of the sample arm matches the reference arm, also known as the zero path length difference.

The scanning pattern and the methods used to process the collected data were based on the OMAG technique,²² which allows the extraction of the 3-D microvascular images. Briefly, an x-y galvo-scanner was used to scan the focused beam spot

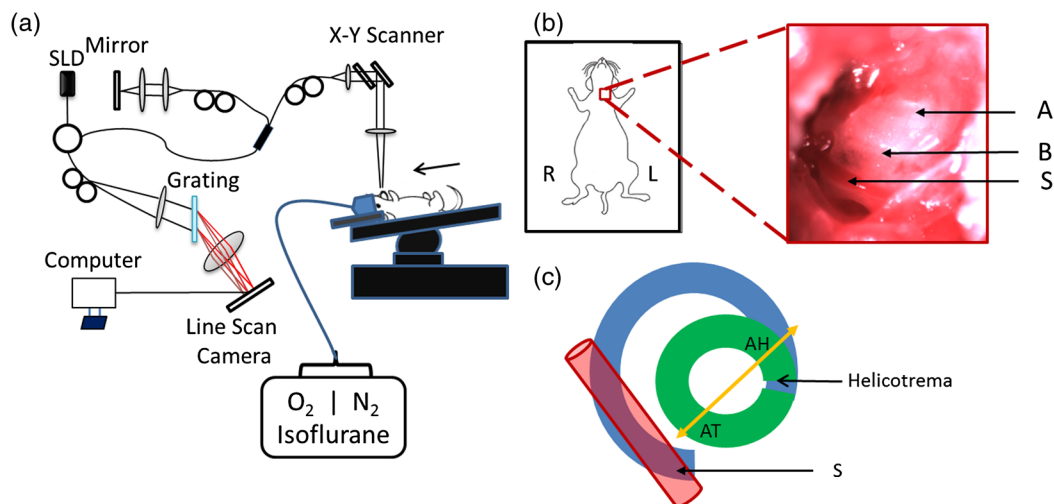


Fig. 1 (a) Experimental setup of the spectral domain optical coherence tomography system (SLD = superluminescent diode). (b) Depiction of the surgical location and picture of the exposed left cochlea of a mouse. The arrows indicate the stapedial artery (S), and the apical (A) and basal (B) turns. This view is the same as used for DOMAG imaging. (c) Schematic diagram of Fig. 1(b) depicting the AT (green), basal turn (blue) and stapedial artery (S). The yellow line with arrow heads indicates the cross-section of the AT regions analyzed by DOMAG imaging, which includes the apical turn proximal to the helicotrema (AH) and the middle of the apical turn (AT).

across the sample, with one scanner moving the beam in the X -direction, and another scanner moving the beam in the Y -direction, as defined by the arrows in Fig. 2. For the experiments presented in this study, the camera had an A-line scan rate of ~ 5 kHz. Each B-scan contained 2000 A-lines that span ~ 1.5 mm.

Before the experiment we acquired a 3-D data set on each animal, which consisted of 240 discrete locations in the Y -direction where 5 B-scans were collected at each location and averaged together. The Y -direction spans a range of ~ 1.5 mm. The system collected two frames per second (fps) by allowing 80% of the time for the mirror to scan the beam, and 20% of the time for the mirror to return to its original position in the X -direction ($5000 \text{ Hz} * 0.8 / 2000$ lines). The data cube of each 3-D image was composed of 1024 by 2000 by 240 ($z-x-y$) voxels. The total acquisition time was 10 minutes ($240 \text{ locations} * 5 \text{ average} / 2 \text{ fps}$).

For the oxygen challenge, we collected 1200 B-scans in the same cross-section position. The total acquisition time was 10 min, which is the duration of the challenge. The 3-D data set enabled us to determine the Doppler angle that was then used to extract the total blood flow on each vessel.

DOMAG is a new method that has been used to calculate the axial blood flow velocity inside vessels. DOMAG has previously been validated by using tissue calibration phantoms, and it has been used for *in vivo* studies of cerebral blood flow.³⁰ The axial flow velocity can be derived from the phase difference between adjacent lines, which is introduced by the

motion of blood cells. The relationship between the phase difference ($\Delta\phi$) and the axial velocity (V_z) is given by:

$$V_z = (\Delta\phi\lambda_0)/(4\pi n\Delta t_A), \quad (1)$$

where λ_0 is the central wavelength of the light source (1310 nm), n is the refractive index of the tissue (~ 1.35) and Δt_A is the time interval between adjacent lines ($1/5000 \text{ Hz} = 200 \mu\text{s}$). The maximum axial velocity that can be measured is ± 1.2 mm/s.

Measurement of the absolute blood flow rate is important in the study of the cochlea, since it allows the evaluation of blood flow dynamics within individual vessels. To obtain the absolute velocity, it is important to determine the angle between the flow velocity vector and the vector of incident OCT light, also known as the Doppler angle. The Doppler angle is determined using the 3-D dataset captured using OMAG.³⁴ The Doppler angle can be calculated using:

$$\Phi = \pi - \arccos[dz/(dx^2 + dy^2 + dz^2)^{1/2}], \quad (2)$$

where dx , dy and dz are the directional components of the blood vessel. The calculation of the total blood flow velocity can be obtained from:

$$V = \text{abs}(V_z / \cos \Phi). \quad (3)$$

Finally, the blood flow rate is determined by:

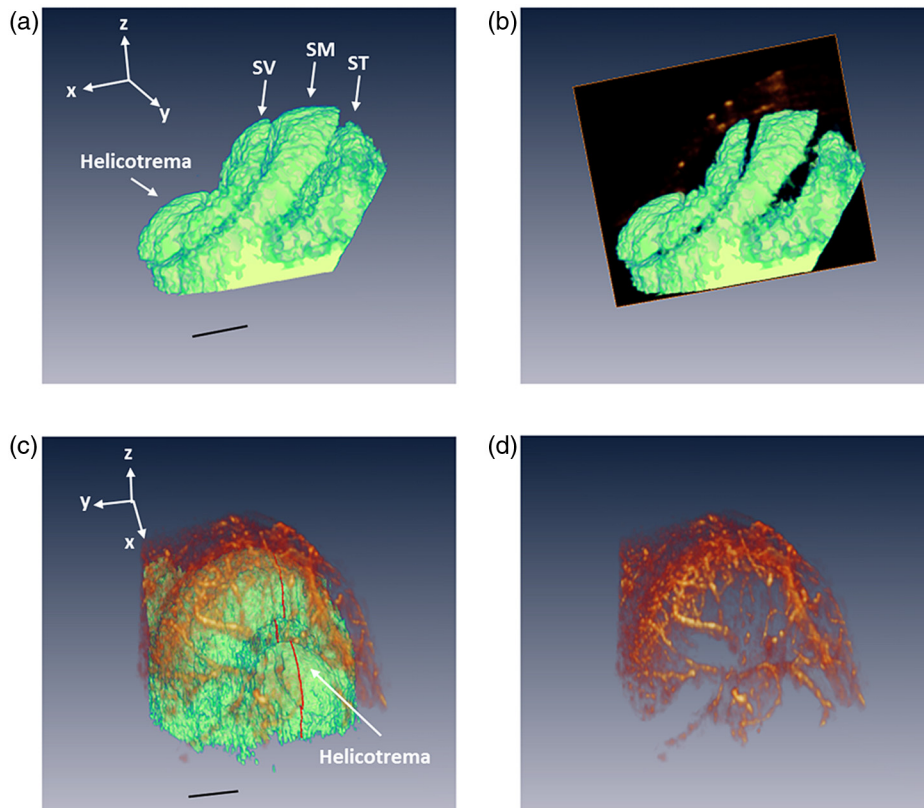


Fig. 2 (a) Three-dimensional side view of the scala media (SM), tympani (ST) and vestibuli (SV), (b) with a cross-section showing the blood vessels obtained with OMAG. The cross-section cuts through the AT and AH, where the helicotrema can be visualized. The OCT light is incident in the z direction. (c) Apex view of the three-dimensional overlap of the cochlear scalas and the blood vessels. (d) Blood vessels alone. The red line through the center plane in (c) corresponds to the same cross-sectional area depicted by the black square in (b). The black line in (a) and (c) represent $250 \mu\text{m}$.

$$\text{Flow} = V \cdot A, \quad (4)$$

where A is the cross-sectional area of the blood vessel.

Given that mice were used as the animal model, we were only capable of measuring the apical turn (AT) *in vivo*, since the SA was blocking the view of the basal turn. Figure 1(c) shows a representation of the cochlea, where the apical and basal turns are presented in green and blue, respectively. The yellow arrow indicates the cochlear cross-section imaged with the OCT, where two regions of the AT are imaged: the middle of the AT and AT proximal to the helicotrema (AH). Note that the SA blocks the view of the basal turn.

Figure 2(a) shows a 3-D side view image of the cochlear scalas of the AT. The scala vestibuli, media and tympani, and the location of the helicotrema (location where the scala tympani and vestibuli meet in the apex) are shown. The image has a cross-section that shows the blood vessels obtained with OMAG [Fig. 2(b)]. Figure 2(c) shows the apex view of the 3-D scalas of the cochlea *in vivo*, overlapped by the 3-D visualization of the blood vessels that enable the determination of the Doppler angle. Figure 2(d) presents the 3-D view of the blood vessels.

2.3 Flow Measurements with Laser Doppler Flowmetry

In this experiment we used a LDF (Periflux PF 2B, Perimed), to calculate the changes in flow within a large volume of the cochlea. The tip of the LDF was placed at the AT. Given that the mouse cochlea is small (~2 mm diameter), we estimate that the LDF averages the changes in flow from several cochlear turns (a hemisphere volume with ~1 to 1.5 mm radius).

2.4 Induction of Hypoxia

After the exposure of the cochlea was completed under 1.5% isoflurane anesthesia with 20% oxygen/80% medical air, the mouse was switched to 20% oxygen/80% nitrogen (normoxia) under 1.5% isoflurane anesthesia prior to the start of the data acquisition. The anesthesia was administered by face mask and the animal was free breathing throughout the cochlear exposure, as well as the hypoxic, challenge. At this time a pulse oximeter (Starr Life Sciences, Oakmont, PA) was placed on the animal to measure the percentage oxygen saturation

(SpO₂). A normoxia baseline was maintained for 3 min at which time the oxygen concentration was lowered approximately by half and the nitrogen was balanced accordingly using a gas-proportioning meter (GMR2, Aalborg, Orangeburg, NY) in order to achieve severe hypoxia (~80%) as determined by the SpO₂ measurements. The hypoxic stimulus was maintained for 4 min followed by a 3-min recovery period in which the oxygen and nitrogen were switched back to normoxic conditions (20% oxygen/80% nitrogen). The flow change was measured in five animals using the DOMAG system and in a separate cohort of five animals using the LDF system. Physiological and LDF measurements were recorded at 1-min intervals while DOMAG measurements were recorded every 0.5 s throughout the 10-min procedure. The mean arterial blood pressure (MABP) was measured with a tail cuff (Kent Scientific, Torrington, CT) in a separate cohort of five animals subjected to the same changes in oxygen concentration but without the surgical procedure that exposes the cochlea.

2.5 Statistical Analysis

Differences in mean MABP among the baseline (3 min), stimulus (4 min) and recovery (3 min) phases were analyzed with one-way ANOVA and post hoc Dunnett's test to compare the MABP of the hypoxia stimulus and the recovery to the baseline MABP which was the control. The data was normally distributed. The criterion for statistical significance was $p < 0.05$. All values for MABP are reported as mean ± standard deviation. Statistical analysis was performed with Prism software.

3 Results

Figure 3(a) presents the mean and standard deviation of the SpO₂ values obtained throughout the challenge in the baseline, stimulus and recovery phases for the DOMAG ($n = 5$), LDF ($n = 5$) and MABP ($n = 5$) cohorts of mice. Severe systemic hypoxia (SpO₂ ~ 80%) was achieved in all the animal cohorts during the stimulus, and the values returned to baseline in the recovery phase.

Figure 3(b) presents the mean and standard deviation of the relative change of MABP obtained from five animals. The change was normalized to the average of the values obtained in the baseline phase. Throughout the challenge there was a decrease in MABP, which did not fully recuperate in the

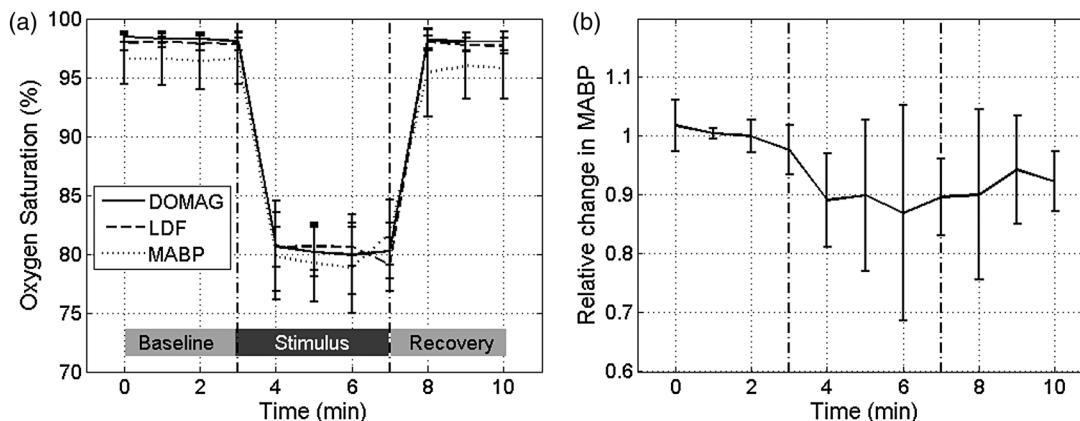


Fig. 3 (a) Mean and standard deviation of the oxygen saturation throughout the experiment for the three cohorts of mice: DOMAG ($n = 5$), LDF ($n = 5$) and MABP ($n = 5$). (b) Mean and standard deviation of the relative change of MABP. The vertical dashed-dot lines indicate the beginning and the ending of the hypoxic stimulus.

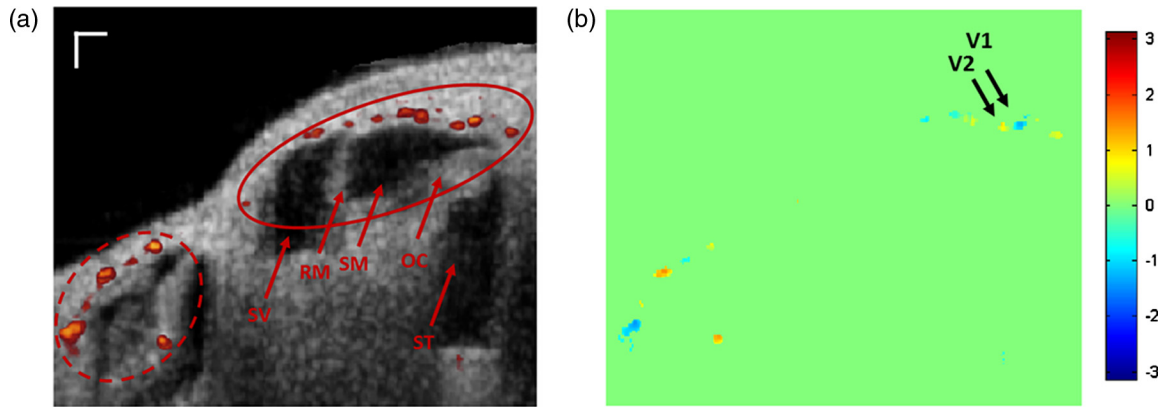


Fig. 4 (a) Structure image of a cross-section of the cochlea including the location of the blood vessels obtained using OMAG. The vessels within the dashed and solid oval correspond to the AH and AT, respectively. The arrows indicate the scala vestibuli (SV), Reissner’s membrane (RM), scala media (SM), organ of Corti (OC) and scala tympani (ST) of the AT. Scale bar: 100 μm . (b) DOMAG image indicating the phase change of the vessels in the axial direction. V1 and V2 are two adjacent vessels with a down and up flow direction, respectively, located in the AT.

recovery phase. The mean and standard deviation of the baseline, stimulus and recovery MABP values within each phase were 78 ± 13 , 67 ± 14 , and 72 ± 10 , respectively.

Figure 4(a) presents a structure image of a cross-section of the cochlea obtained with the OCT system. The red arrows indicate the location of the scala vestibuli, Reissner’s membrane, scala media, organ of Corti and scala tympani, from the AT. The image also shows the location of the blood vessels which have been obtained using OMAG. Two regions for the blood vessels have been selected. The region within the solid

oval contains the blood vessels within the AT, while the region within the dashed oval contains the blood vessels within the AH.

The DOMAG image [Fig. 4(b)] indicates the phase change [proportional to the axial velocity Eq. (1)], which contains values between $-\pi$ and π . The negative and positive values indicate that the blood cells are moving towards the bottom and top of the image, respectively.

In Fig. 5, we observed the average and standard deviation of the changes in CoBF as a function of time from five mice. Three flows were calculated for three regions, the flow in the AH, AT,

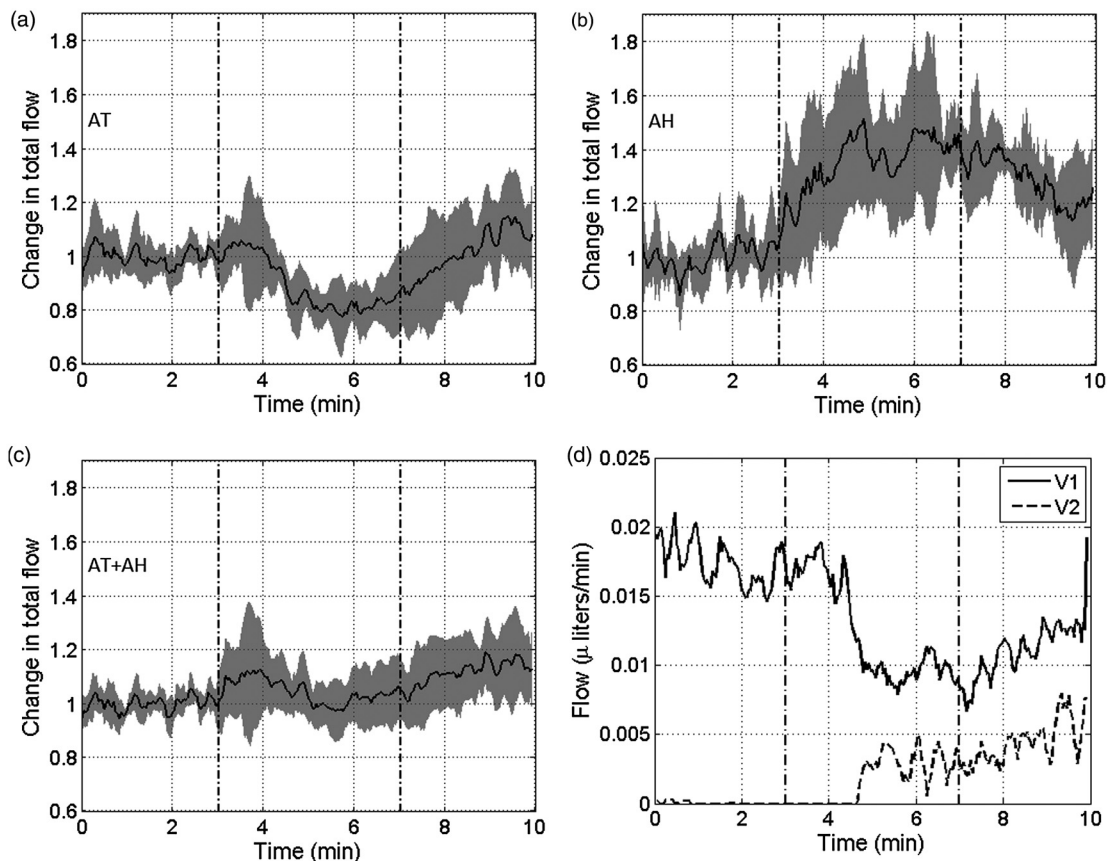


Fig. 5 Changes in cochlear blood flow in the (a) AT, (b) AH, (c) both AT plus AH regions in response to oxygen challenge. (d) Cochlear blood flow for V1 and V2 indicated in Fig. 4(b).

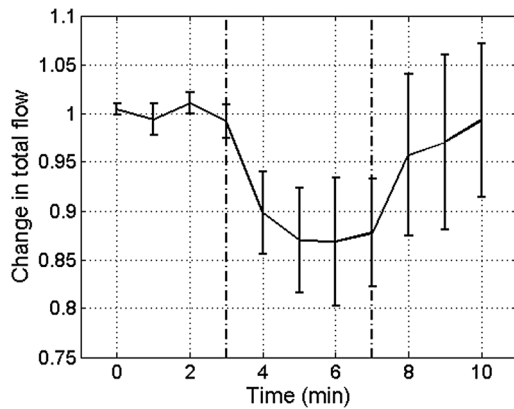


Fig. 6 Changes in cochlear blood flow in response to systemic changes in oxygen concentration measured by LDF ($N = 5$).

and AH plus AT. The flow of each region consisted of the sum of the flow of each vessel within the region. The AH and AT regions have been indicated in Fig. 4(a). The change in flow of each mouse was normalized to the average of the baseline phase. The vessels located in the AT [Fig. 5(a)], present a reduction of CoBF of $\sim 20\%$ during the hypoxia, however, the vessels located in the AH [Fig. 5(b)] present an increase of CoBF of $\sim 40\%$ during the hypoxia. When we take into account the vessels in both regions, we observed a slight increase in CoBF [Fig. 5(c)].

In Fig. 5(d), we present the total flow observed in vessels V1 and V2 [indicated in Fig. 4(b)]. Here we demonstrate that although the vessels in the AT had an average decrease in CoBF of $\sim 20\%$, not all the vessels exhibited the same behavior. The hypoxic stimulus decreased blood flow in V1 yet increased blood flow in V2. Moreover, V2 initially had no flow; however, after the challenge was initiated flow was present.

Figure 6 presents the mean and standard deviation of the change in total flow obtained with the LDF system ($n = 5$). The change in flow of each mouse was normalized to the average of the baseline phase. During hypoxia there was a decrease in blood flow of approximately 13%. After the hypoxia was terminated and the oxygen levels were restored to normal, the average LDF returned to baseline.

4 Discussion

This study demonstrated that DOMAG could distinguish changes in CoBF within the AH and AT in response to systemic hypoxia. From Fig. 2 we can observe that OCT and OMAG enabled the 3-D visualization of the turns inside the cochlea and the location of the blood vessels. The cochlea in mice has one and three-quarter turns consisting of the apical and basal turn.³⁵ Given that mice were used as the animal model, it was challenging to obtain images from the basal turn since the OCT beam was blocked by the SA, and also the basal turn was located at a higher depth from the OCT beam focal point. We did, however, collect reliable images *in vivo* of two areas of the AT [AH and AT, indicated in Fig. 1(c)]. Since the 3-D images of the cochlea microvasculature were obtained [Fig. 2(c) and 2(d)], it was possible to determine the Doppler angle of each vessel, and calculate the total velocity and flow [Eqs. (3) and (4)] using the DOMAG method. We speculate that if DOMAG would be capable of measuring a larger volume of the cochlea (i.e., including the basal turn), we would

observe a total decrease in CoBF within the whole cochlea; however, since we are currently limited to the AT, we observed a slight increase [Fig. 5(c)]. In future studies we plan to improve the surgical procedure in mice or use a different animal model which would better enable us to visualize both cochlea turns.

Figure 5 presents the changes in blood flow from two areas of the AT (AH and AT). It is interesting to observe that there was an increase in CoBF in the AH while the AT had a decrease. This was an unexpected result but was consistent among all five animals subjected to systemic hypoxia. We hypothesize that there may be a hierarchy in blood flow for different turns and vascular areas of the turns. It is important to mention that to obtain the changes in CoBF in Fig. 5, two regions were manually selected [Fig. 4(a)]. The selection of the regions may have some error, given that the vessels included in the region were chosen by the investigators according to their prominence in the image.

In Figs. 5 and 6, there was an increase in the standard deviation after the hypoxia was initiated. This indicates that not all animals had the same reaction to the challenge. Although the magnitude of the CoBF change had animal to animal variability, an increase/decrease CoBF was observed during the systemic hypoxia in the AH/AT regions of the AT in all five animals measured by the DOMAG method.

Since CoBF is a function of cochlear perfusion pressure, which is calculated as the difference between the MABP and the inner ear fluid pressure, a drop in MABP would result in decreased CoBF as determined by LDF.³⁶ In our current study, the baseline MABP was within the normal range³⁷ and although the decrease in MABP during systemic hypoxia was not significant, we cannot rule out that a small decrease in MABP may have an effect on a decrease in CoBF as we did not measure the cochlear perfusion pressure. We previously observed that systemic hypoxia decreases cerebral blood flow,³⁸ and we expected a similar reduction for CoBF. Our results using LDF are in agreement with these previous observations as we detected a drop in CoBF and MABP during hypoxia.^{38,39} However, the results obtained from DOMAG imaging suggest that CoBF responses to hypoxia are more complex.

Figure 5(d) shows an example of two adjacent vessels located in the same region which had different responses to the hypoxia. This figure demonstrates the advantage of the DOMAG method over LDF, where single vessel resolution and absolute blood flow values can be determined. V2 initially has no flow, but when the challenge is initiated, it becomes active, which could be an indication of vessel recruitment. These data highlight the importance of DOMAG, which can determine the effect of systemic hypoxia in different regions of the cochlea. This technical advance will allow further understanding of the intricacies of CoBF.

The method used to acquire the data is sensitive to red blood cell velocities that are higher than $160 \mu\text{m/s}$ in the axial direction. The average axial velocities measured in this paper were $300 \mu\text{m/s}$. We have previously demonstrated a technique that allows the acquisition of red blood cell velocities as low as $4 \mu\text{m/s}$,³² using a different scanning pattern, which would also allow the acquisition of the 3-D image within a few seconds. We plan to improve this scanning pattern such that it can be applicable for cochlea imaging.

5 Conclusions

In this study we have demonstrated that the changes in CoBF during hypoxia increased at the AH and decreased at the AT.

Also, DOMAG enabled the determination of the total blood flow of individual vessels, where it was observed that adjacent blood vessels can have different responses to a hypoxic challenge. Understanding the pathophysiology of blood flow will advance our ability to study the relationship between blood flow and hearing loss to improve diagnosis and treatment strategies for hearing disorders.

Acknowledgments

This work was supported in part by research grants from the National Institutes of Health (R01DC01201, R01DC00105, P30DC005983). The content is solely the responsibility of the authors and does not necessarily represent the official views of the grant-giving bodies.

References

- Primary Ear and Hearing Care Training Resource: Advanced Level, World Health Organization, Geneva, Switzerland (2006).
- T. Nakashima et al., "Disorders of cochlear blood flow," *Brain Res. Rev.* **43**(1), 17–28 (2003).
- A. L. Nuttall, "Sound-induced cochlear ischemia/hypoxia as a mechanism of hearing loss," *Noise Health* **2**(5), 17–32 (1999).
- C. Aimoni et al., "Hearing threshold assessment in young children with electrocochleography (EcochG) and auditory brainstem responses (ABR): experience at the University Hospital of Ferrara," *Auris, Nasus, Larynx* **37**(5), 553–557 (2010).
- P. Mitchell et al., "Relationship of Type 2 diabetes to the prevalence, incidence and progression of age-related hearing loss," *Diabetic Med.* **26**(5), 483–488 (2009).
- J. T. Y. Chou and K. Rodgers, "Respiration of tissues lining the mammalian membranous labyrinth," *J. Laryngol. Otol.* **76**(5), 341–351 (1962).
- H. Haupt, F. Scheibe, and C. Ludwig, "Changes in cochlear oxygenation, microcirculation and auditory function during prolonged general hypoxia," *European Arch. Oto-Rhino-Laryngol.* **250**(7), 396–400 (1993).
- R. Thalmann, T. Miyoshi, and I. Thalmann, "The influence of ischemia upon the energy reserves of inner ear tissues," *Laryngoscope* **82**(12), 2249–2272 (1972).
- P. R. Thorne and A. L. Nuttall, "Laser doppler measurements of cochlear blood flow during loud sound exposure in the guinea pig," *Hear. Res.* **27**(1), 1–10 (1987).
- A. L. Nuttall, "Techniques for the observation and measurement of red blood cell velocity in vessels of the guinea pig cochlea," *Hear. Res.* **27**(2), 111–119 (1987).
- J. M. Miller, N. J. Marks, and P. C. Goodwin, "Laser Doppler measurements of cochlear blood flow," *Hear. Res.* **11**(3), 385–394 (1983).
- P. C. Goodwin et al., "The laser Doppler: a non-invasive measure of cochlear blood flow," *Acta Oto-Laryngol.* **98**(5–6), 403–412 (1984).
- H. Yamamoto et al., "Contribution of stapedial artery to blood flow in the cochlea and its surrounding bone," *Hear. Res.* **186**(1–2), 69–74 (2003).
- M. Tominaga et al., "Response of cochlear blood flow to prostaglandin E1 applied topically to the round window," *Acta Oto-Laryngol.* **126**(3), 232–236 (2006).
- P. R. Thorne et al., "Sound-induced artifact in cochlear blood flow measurements using the laser Doppler flowmeter," *Hear. Res.* **31**(3), 229–234 (1987).
- T. J. Ffytche et al., "Effects of changes in intraocular pressure on the retinal microcirculation," *Br. J. Ophthalmol.* **58**(5), 514–522 (1974).
- R. Leitgeb et al., "Real-time assessment of retinal blood flow with ultra fast acquisition by color Doppler Fourier domain optical coherence tomography," *Opt. Express* **11**(23), 3116–3121 (2003).
- S. Makita et al., "Optical coherence angiography," *Opt. Express* **14**(17), 7821–7840 (2006).
- A. Szkulmowska et al., "Three-dimensional quantitative imaging of retinal and choroidal blood flow velocity using joint spectral and time domain optical coherence tomography," *Opt. Express* **17**(13), 10584–10598 (2009).
- Y. K. Tao, A. M. Davis, and J. A. Izatt, "Single-pass volumetric bidirectional blood flow imaging spectral domain optical coherence tomography using a modified Hilbert transform," *Opt. Express* **16**(16), 12350–12361 (2008).
- B. J. Vakoc et al., "Phase-resolved optical frequency domain imaging," *Opt. Express* **13**(14), 5483–5493 (2005).
- R. K. Wang, "Optical microangiography: a label free 3D imaging technology to visualize and quantify blood circulations within tissue beds *in vivo*," *IEEE J. Sel. Topics Quantum Electron.* **16**(3), 545–554 (2010).
- R. K. Wang and S. Hurst, "Mapping of cerebro-vascular blood perfusion in mice with skin and skull intact by optical micro-angiography at 1.3 μm wavelength," *Opt. Express* **15**(18), 11402–11412 (2007).
- L. An and R. K. Wang, "In vivo volumetric imaging of vascular perfusion within human retina and choroids with optical micro-angiography," *Opt. Express* **16**(15), 11438–11452 (2008).
- N. Choudhury et al., "Volumetric imaging of blood flow within cochlea in gerbil *in vivo*," *IEEE J. Sel. Topics Quantum Electron.* **16**(3), 524–529 (2010).
- H. M. Subhash et al., "Volumetric *in vivo* imaging of intracochlear microstructures in mice by high-speed spectral domain optical coherence tomography," *J. Biomed. Opt.* **15**(3), 036024 (2010).
- H. M. Subhash et al., "Volumetric *in vivo* imaging of microvascular perfusion within the intact cochlea in mice using ultra-high sensitive optical microangiography," *IEEE Trans. Med. Imag.* **30**(2), 224–230 (2011).
- Z. Chen et al., "Noninvasive imaging of *in vivo* blood flow velocity using optical Doppler tomography," *Opt. Lett.* **22**(14), 1119–1121 (1997).
- Y. Zhao et al., "Real-time phase-resolved functional optical coherence tomography by use of optical Hilbert transformation," *Opt. Lett.* **27**(2), 98–100 (2002).
- R. K. Wang and L. An, "Doppler optical micro-angiography for volumetric imaging of vascular perfusion *in vivo*," *Opt. Express* **17**(11), 8926–8940 (2009).
- J. Jero et al., "A surgical approach appropriate for targeted cochlear gene therapy in the mouse," *Hear. Res.* **151**(1–2), 106–114 (2001).
- L. An, J. Qin, and R. K. Wang, "Ultrasound sensitive optical microangiography for *in vivo* imaging of microcirculations within human skin tissue beds," *Opt. Express* **18**(8), 8220–8228 (2010).
- A. F. Fercher et al., "Optical coherence tomography—principles and applications," *Rep. Prog. Phys.* **66**(2), 239–303 (2003).
- Z. Zhi et al., "Volumetric and quantitative imaging of retinal blood flow in rats with optical microangiography," *Biomed. Opt. Express* **2**(3), 579–591 (2011).
- R. Cantos et al., "Patterning of the mammalian cochlea," *Proc. Natl. Acad. Sci. U. S. A.* **97**(22), 11707–11713 (2000).
- T. Nakashima, A. L. Nuttall, and J. M. Miller, "Effects of vasodilating agents on cochlear blood flow in mice," *Hear. Res.* **80**(2), 241–246 (1994).
- M. Uchida et al., "Dose-dependent effects of androgens on outcome after focal cerebral ischemia in adult male mice," *J. Cereb. Blood flow Metab.* **29**, 1454–1462 (2009).
- Y. Jia, P. Li, and R. K. Wang, "Optical microangiography provides an ability to monitor responses of cerebral microcirculation to hypoxia and hyperoxia in mice," *J. Biomed. Opt.* **16**(9), 096019 (2011).
- T. Tono et al., "Effects of trimetaphan-induced deliberate hypotension on human cochlear blood flow," *Acta Oto-Laryngol.* **118**, 40–43 (1998).